Frequency-dependent power output and skeletal muscle design

Article *in* Comparative Biochemistry and Physiology - Part A Molecular & Integrative Physiology · March 2009

DOI: 10.1016/j.cbpa.2008.11.021 · Source: PubMed

2 authors:

Scott Medler
St. Bonaventure University
38 PUBLICATIONS **650** CITATIONS
SEE PROFILE

Kevin Hulme
University at Buffalo, The State University of New York
90 PUBLICATIONS **755** CITATIONS
SEE PROFILE

Comparative Biochemistry and Physiology, Part A 152 (2009) 407–417

Contents lists available at ScienceDirect

Comparative Biochemistry and Physiology, Part A

journal homepage: www.elsevier.com/locate/cbpa

Frequency-dependent power output and skeletal muscle design

Scott Medler [a,*], Kevin Hulme [b]

[a] Department of Biological Sciences, University at Buffalo, Buffalo, NY 14260, United States
[b] New York State Center for Engineering Design and Industrial Innovation (NYSCEDII), University at Buffalo, Buffalo, NY 14260, United States

ARTICLE INFO

Article history:
Received 1 July 2008
Received in revised form 12 September 2008
Accepted 16 November 2008
Available online 6 December 2008

Keywords:
Skeletal muscle
Power output
Frequency
Resonance
Locomotion
Computational model

ABSTRACT

Cyclically contracting muscles provide power for a variety of processes including locomotion, pumping blood, respiration, and sound production. In the current study, we apply a computational model derived from force–velocity relationships to explore how sustained power output is systematically affected by shortening velocity, operational frequency, and strain amplitude. Our results demonstrate that patterns of frequency dependent power output are based on a precise balance between a muscle's intrinsic shortening velocity and strain amplitude. We discuss the implications of this constraint for skeletal muscle design, and then explore implications for physiological processes based on cyclical muscle contraction. One such process is animal locomotion, where musculoskeletal systems make use of resonant properties to reduce the amount of metabolic energy used for running, swimming, or flying. We propose that skeletal muscle phenotype is tuned to this operational frequency, since each muscle has a limited range of frequencies at which power can be produced efficiently. This principle also has important implications for our understanding muscle plasticity, because skeletal muscles are capable of altering their active contractile properties in response to a number of different stimuli. We discuss the possibility that muscles are dynamically tuned to match the resonant properties of the entire musculoskeletal system.

1. Introduction

Striated muscles often operate through cyclical contractions, providing the power to drive a variety of physiological processes including diverse modes of locomotion, pumping of blood, powering respiration, and sound production. The highly conserved nature of striated muscles frequently leads to common design principles and constraints in the operation of otherwise seemingly diverse processes. One important example of this is the principle that cyclically contracting muscles generate maximal sustained power at a unique contractile frequency (Altringham and Young, 1991; Johnson et al., 1993; Swoap et al., 1993; Askew and Marsh, 1997; Josephson, 1997; Swoap et al., 1997; Harwood et al., 1998; Shiels et al., 1998; Josephson et al., 2000b; Syme and Shadwick, 2002). This is an important principle, because many physiological processes are driven by skeletal muscle motors at specific frequencies, but the far-reaching implications for a variety of integrated processes have not been fully appreciated (Full, 1997; Daniel and Tu, 1999; Dickinson et al., 2000; Ahlborn et al., 2006; Holmes et al., 2006). A case in point, musculoskeletal systems possess resonant properties that limit their range of operational frequencies, and when an animal can 'tune' to the resonant frequency of operation the costs of locomotion are minimized (Ahlborn and Blake, 2002; Ahlborn et al., 2006). For these systems to work effectively, the muscles powering these processes must also be 'tuned' to produce power at the frequency of operation. To date, no studies have explored how skeletal muscle organization might be shaped by these frequency-dependent processes. In the current study, we applied a computational model of sustained muscle power output to examine some of the principles of muscle design that effect power output at different operational frequencies.

Several different factors affect muscle power output, including the force–velocity relationship, the kinetics of activation and deactivation, the length–tension relationship, and others (Rome and Lindstedt, 1997; Josephson, 1999; Marsh, 1999; Caiozzo, 2002). In this study, we focus exclusively on the force–velocity relationship and its influence on power output at different operational frequencies and strain amplitudes. This limited focus is important for the following reasons. First, the other above factors, including muscle activation and deactivation, have the effect of limiting power output (Marsh, 1990; Caiozzo and Baldwin, 1997; Caiozzo, 2002). By focusing exclusively on the force–velocity relationship and treating muscle activation and deactivation as instantaneous, we can explore the theoretical limits to power output as a function of operational frequency (Caiozzo, 2002). In real-world muscles, these limits are generally not attained, but represent an upper ceiling of power output that reveals a number of patterns and constraints of muscle operation. Second, the large number of parameters potentially affecting muscle operation is extensive and their interactions can be complex (Josephson, 1999; Marsh, 1999; Caiozzo, 2002). Moreover, there are already comprehensive reviews that consider these parameters more fully (Rome and Lindstedt, 1997; Josephson, 1999; Caiozzo, 2002). Finally, the force–velocity relationship is primarily determined by the myosin heavy chain (MHC) isoform(s) operating

* Corresponding author. Tel.: +1 716 645 2363x201; fax: +1 716 645 2975.
E-mail address: smedler@buffalo.edu (S. Medler).

1095-6433/$ – see front matter © 2008 Elsevier Inc. All rights reserved.
doi:10.1016/j.cbpa.2008.11.021

within a particular muscle (Schiaffino and Reggiani, 1996; Caiozzo, 2002). This means that many of the general trends we identify here can be linked directly to the molecular design of the muscle. Specifically, changes in MHC isoform expression can be linked mechanistically to the ability of a muscle to dynamically alter its contractile properties to match the resonant properties of the musculoskeletal system.

In the current study, we apply our computational model of sustained muscle power output to explore the relationship between a muscle's intrinsic shortening velocity, operating frequency, muscle strain, and power output. We compare predicted patterns of muscle operation with data from a diverse group of muscles used by a wide array of animals for locomotion and sound production. This analysis explains a number of important patterns, including the observation that operational frequency is directly proportional to the ratio of muscle shortening velocity and strain amplitude. We then explore how the model can be applied to specific case studies of muscle function by modeling human muscle function and the scaling of intrinsic muscle shortening velocity in quadrupedal mammals. Our goal here is not only to draw general conclusions about muscle design, but also to demonstrate how this model can be applied to a number of different case studies. Finally, we discuss the implications of our observations for several processes including resonance in locomotion, limits to athletic performance, and skeletal muscle plasticity.

2. Materials and methods

2.1. Computational model

We developed a computational model based on the ideas originally presented by Weis-Fough and Alexander (Weis-Fough and Alexander, 1977), and later developed more fully by Josephson (1985a). The basic concept of the model is to measure the sustained power output from a simulated muscle using the work-loop method (Josephson, 1985a). Muscle force and length are determined for each point of a contraction cycle, and the enclosed loop is equal to the work done per cycle. In the current model, muscle activation and deactivation are treated as instantaneous and the sustained power output is simply the product of the work per cycle and the cycle frequency. This approach has been used by other investigators for a number of different specific applications (Josephson, 1989; Caiozzo and Baldwin, 1997; Askew and Marsh, 1998). In the current study, we applied this model to study the systematic relationship between intrinsic shortening velocity, operational frequency, strain amplitude, and sustained power output.

The determination of muscle force as a function of shortening velocity is derived from the Hill equation. The Hill model (1938) is a well-known state equation applicable to skeletal muscle that has been stimulated, and relates force to velocity. Parametric analysis of this model serves as the motivational cornerstone for the development of our computational model. The Hill equation is:

$$(V + b)(P + a) = b(Po + a) \quad (1)$$

where P is the load or tension in the muscle, V is the velocity of contraction, P_0 is the maximum load or tension generated in the muscle, a and b are constants with units of force and velocity, respectively.

Hill's equation demonstrates that the relationship between P and V, is hyperbolic: the higher the load applied to the muscle, the lower the contraction velocity; the higher the contraction velocity, the lower the tension in the muscle. The ratio of a/Po describes the relative curvature of the Hill equation, with lower values of the relationship defining a greater degree of curvature and higher values producing more of a straight line. Typical values of a/Po are in the range 0.25, although they vary considerably among different muscles (Josephson, 1993). For most of our simulations, we set a/Po at a value of 0.30. We used the parameter 'b' to adjust the maximum shortening velocity, as previously discussed by Josephson (Josephson, 1989). For modeling purposes, we varied the maximum shortening velocity from 1 to 20 muscle lengths per second (L/s), which generally represents the range of values observed for real muscles (Josephson, 1993; Medler, 2002). Maximum tetanic tension was given a relative, unitless value (0–10), so that the power output is also relative. The general shape of these relationships is shown in Fig. 1.

Muscle length as a function of time is defined by the specific strain trajectory input into the simulation. At any moment, instantaneous muscle length is described as:

$$L = A \sin(\mathrm{wt}) \quad (2)$$

where L is muscle length, A is the amplitude of the sine wave, w is angular velocity, and t is time (Caiozzo and Baldwin, 1997; Askew and Marsh, 1998). Instantaneous velocity is determined as the derivative of muscle length (Eq. (2)) over time and is used in conjunction with a particular Hill equation (Caiozzo and Baldwin, 1997; Askew and Marsh, 1998) simply as:

$$V = -wA \cos(\mathrm{wt}) \quad (3)$$

The term on the right is negative here because by convention, muscle shortening velocity is considered to be positive when the muscle is decreasing in length. The instantaneous velocity is then applied to the specific Hill equation of interest (Eq. (1)) and the muscle force is determined. Instantaneous force was determined for hundreds of time points

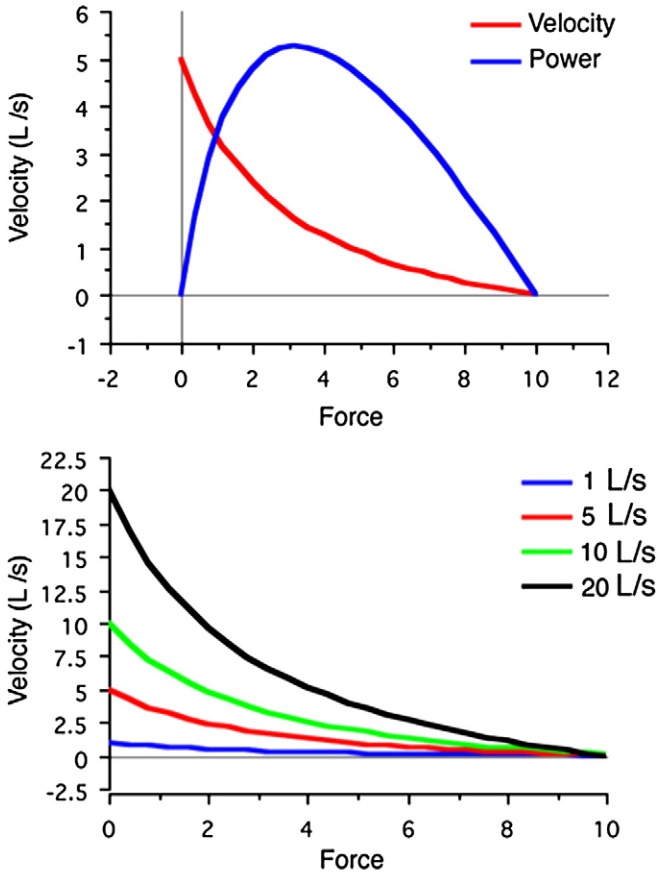

Fig. 1. Modeled force–velocity relationships used in the current study. A. Single force–velocity curve and corresponding instantaneous power output. Shortening velocity has units of muscle lengths per second (L/s), while force is relative and is, therefore, unitless. Maximum instantaneous power output is produced at approximately 30% of the maximum isometric force. B. Family of force–velocity curves with different maximum shortening velocities. Shortening velocity was adjusted by changing the parameter 'b' in the Hill equation, and maximum shortening velocities were modeling from 1 to 20 L/s.

within each shortening cycle and the work per cycle was estimated by summation of the force values over the entire cycle, with corresponding muscle length being estimated from Eq. (2). Sustained power output was then estimated as the product of work per cycle and the operational frequency. Strain amplitude was controlled in our simulations by adjusting the values of A, and frequency (f) was controlled through changes in w ($f=w/2\pi$). Calculations of sustained power output were performed using a computer program (and Graphical User Interface) written in C++ (Stroustrup, 1987; Kernighan and Ritchie, 1988) for a personal computer running with Windows. A copy of our model written in this code can be provided to those interested in developing their own model.

Table 1
Operational frequency, strain amplitude, and shortening velocity for diverse cyclically contracting muscles

Species	Common name	Muscle	Freq (Hz)	Strain* (L)	Vel (L*s^{-1})
Mammal					
Mus musculus[1]	mouse	EDL	12.0	0.131	4.2
		soleus	5.0	0.108	1.8
Rattus norvegicus[2]	rat	plantaris	6.0	0.089	1.6
		soleus	1.5	0.182	0.7
Canis familiaris[3]	dog	triceps	3.0	0.150	2.3
		SM	3.0	0.054	0.9
		VL	2.8	0.153	3.0
Capra hircus[4]	goat	VL	2.8	0.430	2.0
		biceps	2.8	0.300	2.1
Equus caballus[5]	horse	triceps	1.7	0.103	0.8
		VL	1.7	0.081	0.7
Bird					
Taeniopygia guttata[6]	zebra finch	pectoralis	30.0	0.160	7.9
Coturnix chinensis[7]	quail	pectoralis	23.2	0.234	7.8
Colinus virginianus[8]	bobwhite	pectoralis	19.9	0.190	5.9
Alectoris chuckar[8]	chukar	pectoralis	16.1	0.228	6.3
Melopsitaccus undulatus[6]	budgerigars	pectoralis	16.0	0.150	4.1
Sturnus vulgaris[9]	starling	pectoralis	15.0	0.215	6.7
Phasianus colchicus[8]	pheasant	pectoralis	11.0	0.222	4.3
Anas platyrhynchos[10]	mallard	pectoralis	9.0	0.360	4.8
Columba livia[11]	pigeon	AP	8.7	0.320	5.4
		PP	8.7	0.320	4.9
Meleagris gallopavo[8]	turkey	pectoralis	7.6	0.350	4.8
Reptile					
Crotalus atrox[12]	rattlesnake	tailshaker	100.0	0.020	4.0
Dipsosaurus dorsalis[13]	desert iguana (5 g)	IF	18.8	0.120	7.7
	desert iguana (50 g)	IF	11.8	0.120	6.5
Amphibian					
Hyla chrysoscelis[14]	tree frog	EO	44.0	0.080	5.9
Hyla versicolor[14]	tree frog	EO	21.0	0.120	3.4
Fish					
Opsanus tau[15]	toadfish	swimbladder	22.0§	0.020	4.0
		red	0.8	0.150	1.2
		white	4.0	0.060	0.8
Gadus morhua[16]	cod (10 cm)	hypaxial	13.5	0.093	2.8
	cod (60 cm)	hypaxial	5.4	0.050	0.7
Scorpaena notata[17]	scorpion fish	white	10.9	0.140	5.1
Stenotomus chrysops[18]	scup	pink	6.8	0.070	2.4
		red	5.0	0.070	1.8
Mollusk					
Argopecten irradians[19]	scallop	adductor	1.8	0.230	0.7
Crustacean					
Carcinus maenus[20]	crab	flagellar	10.0	0.057	2.2
Ocypode quadrata[21]	ghost crab	EC	6.0	0.116	1.4
		FC	6.0	0.176	1.7
Insect					
Drosophila virilis[22]	fruitfly	DVM	166.0	0.033	11.0
		DLM	161.0	0.035	11.3
Bombus terrestris[23]	bumble bee	dorsoventral	125.0	0.020	6.0
Neoconocephalus triops[24]	tettigoniid insect	metathoracic	100.0	0.020	4.6
		metathoracic	25.0	0.060	3.1
Cotinus mutablis[25]	beetle	basalar	94.0	0.050	9.4
Cyclochila australasiae[26]	cicada	tymbal	75.0	0.039	5.9
Libellula pulchella[27]	dragonfly	basalar	37.0	0.100	3.0
Schistocerca gregaria[28]	locust	metathoracic	20.0	0.040	1.6
Blaberus discoidalis[29]	roach	mesothoracic	8.0	0.120	1.7
		metathoracic	8.0	0.164	2.1

Notes to table
*Strain is total strain (ie, 0.25=±0.125 L).
§ The toadfish swimbladder muscle is capable of producing power at up to 200 Hz, but maximum power is generated at 22 Hz.
L=muscle length; EDL=extensor digitorum longus; SM=semimembranosus; VL=vastus lateralis; AP=anterior region of pectoralis; PP=posterior region of pectoralis; IF=iliofibularis muscle; EO=external oblique; EC=the extensor carpopodite muscle; FC=the flexor carpopodite muscle; DVM=dorso-ventral muscles; DLM=dorso-longitudinal muscles.
[1] (James et al., 1995; Askew and Marsh, 1997); [2] (Swoap et al., 1997); [3] (Carrier et al., 1998; Gregersen et al., 1998); [4](Gillis et al., 2005); [5] (Hoyt et al., 2005); [6] (Ellerby and Askew, 2007); [7] (Askew and Marsh, 2001); [8] (Tobalske and Dial, 2000); [9](Biewener et al., 1992); [10] (Williamson et al., 2001b); [11] (Biewener et al., 1998); [12] (Rome et al., 1996); [13] (Marsh, 1988; Swoap et al., 1993); [14] (Girgenrath and Marsh, 1999); [15] (Rome et al., 1996; Young and Rome, 2001); [16](Anderson and Johnston, 1992); [17](Wakeling and Johnston, 1998); [18] (Coughlin et al., 1996); [19] (Marsh and Olson, 1994); [20] (Josephson and Stokes, 1994); [21] Perry et al., in press; [22] (Chan and Dickinson, 1996); [23] (Josephson and Ellington, 1997); [24] (Josephson, 1985b); [25] (Josephson et al., 2000b); [26] (Bennet-Clark and Daws, 1999); [27] (Fitzhugh and Marden, 1997; Marden et al., 2001); [28] (Mizisin and Josephson, 1987); [29] (Full et al., 1998).

2.2. Modeling muscle power output

We used the model to explore systematic patterns of sustained power output as a function of frequency, strain amplitude, intrinsic shortening velocity, and relative muscle force. For each muscle, sustained power output was recorded as frequency was varied from 1–50 Hz and the total strain amplitude was varied from 1–30% (±0.5% to ±15%) of rest length. In a meta-analysis of available published data, we compared our results for systematic patterns of muscle power output with biological data that included operational frequency, strain amplitude, and shortening velocity from a group of muscles from 34 diverse species including mammals, birds, fish, lizards, insects, and mollusks (Table 1). Unifying this diverse group of muscles is the common role of sustained power production through cyclical contractions, whether the muscles are used for running, swimming, flying, or sound production. Some of these data were collected *in vivo*, from animals operating during locomotion, while others were determined from isolated muscles using the work loop technique. When shortening velocity was only reported as V_{max}, average velocities were estimated to be 30% of maximum. Collectively, these data provide a wide range of values for operational frequency (0.8–166 Hz), total muscle strain (0.02–0.43 fiber length), and shortening velocity (0.66–11.3 length/s). The data set includes both synchronous and asynchronous muscles.

In addition to the general modeling of power output across a range of frequencies and strain amplitudes, we also used the model to make predictions about specific case examples. In one of these, we modeled the power output from human muscle fiber types (I, IIA, and IIX) at different operational frequencies. Maximum shortening velocities for these fiber types were taken from published data from isolated fibers as I: 0.35 L/s; IIA: 1.07 L/s; IIX: 3.68 L/s (Larsson and Moss, 1993; Medler, 2002), but adjusted for physiological temperature using the Q_{10} values reported by Lionikas et al. (2006) to yield: I: 1.6 L/s; IIA: 4.4 L/s; IIX: 12.9 L/s. Strain amplitude was set to 8%, which is approximately the degree of muscle fascicle shortening during running in human subjects (Ishikawa et al., 2007). We were also interested in muscle scaling effects and in predicting how a muscle's shortening velocity could evolve to match operational frequency in different sized mammals. We used the frequencies of muscle contraction at the trot to gallop transition reported by Heglund et al. (1974) to predict the corresponding muscle shortening velocities that would maximize power output. These frequencies were estimated from Fig. 1 in Heglund et al. (1974) to be: mouse: 7.75 Hz; rat: 5 Hz; dog: 3.75 Hz; horse: 2.25 Hz. Strain amplitude was treated as a constant (10% total strain) for each species.

2.3. Statistical analyses

Data output from the computer model were imported into a statistical software package (Statview+Graphics, SAS Institute) and used for graphics and statistical analyses. Most of the statistical analyses were limited to patterns in the biological data compiled in Table 1, and included power regression analyses of muscle strain and shortening velocity as a function of operational frequency. In one analysis, the data were partitioned according to the estimated V_{max} (<5, 5–10, 10–20, or >20 L/s) and individual power curves were fit to the data. We also performed a linear regression analysis on the ratio between shortening velocity and strain amplitude as a function of operational frequency. Because of potential problems inherent in the analysis of ratios (Packard and Boardman, 1999), we performed an alternate multiple regression analysis of the same data with log frequency as the dependent variable and log strain amplitude and log shortening velocity as the independent variables. For analysis of the effects of body size on contractile properties, linear regression analysis was used with either log stride frequency or log V_{max} were fit as a function of log body mass. For all regression analyses statistical significance was accepted at $\propto$=0.05.

3. Results

3.1. General relationships

When power output was estimated as a function of both frequency and amplitude, a simple pattern was observed. Sustained power output exhibited a convex surface, whose peak followed a curved line with respect to strain amplitude and operational frequency (Fig. 2). Increasing muscle force increased the amplitude of this peak, but the limits of power production with respect to frequency and amplitude remained unchanged (data not shown). For a given intrinsic shortening velocity (V_{max}), the peak of the power surface followed a line where frequency and strain amplitude were inversely proportional. As V_{max} increased, the curve demarking the peak of the power surface was shifted upward and toward the center of the graph, so that a family of curves was produced, with each curve corresponding to a specific muscle shortening velocity (Fig. 2B).

Plotting experimental data from a variety of power producing muscles (Table 1) demonstrated that the operating parameters of these muscles conformed to this general relationship (Fig. 2C). A regression line through these data was described by strain=0.22* frequency$^{-0.31}$, and when categorized by V_{max} the data fit the pattern shown in 2B. In an alternate analysis, we performed a multiple regression and found the significant relationship: frequency=0.43* strain$^{-0.83}$* velocity$^{1.28}$ (p<0.0001). This relationship confirms that frequency is directly proportional to muscle shortening velocity, but inversely proportional to strain amplitude.

The above relationships demonstrated that power output is a systematic function of operational frequency, amplitude, and muscle shortening velocity. However, when strain amplitude was not factored into this relationship, there was not a linear correlation between muscle shortening velocity and operational frequency (Fig. 3A). In the most general sense, the line demarcating maximum power output exhibited a reciprocal relationship between strain amplitude and operational frequency (Fig. 2A and B). The elevation of this line was proportional to the shortening velocity V_{max} of the muscle, with faster muscles having a greater elevation (Fig. 2B and C). Log transforming both the amplitude and frequency axes in this regression yielded parallel lines with a slope of −1, and the elevation being determined by the V_{max} (not shown).

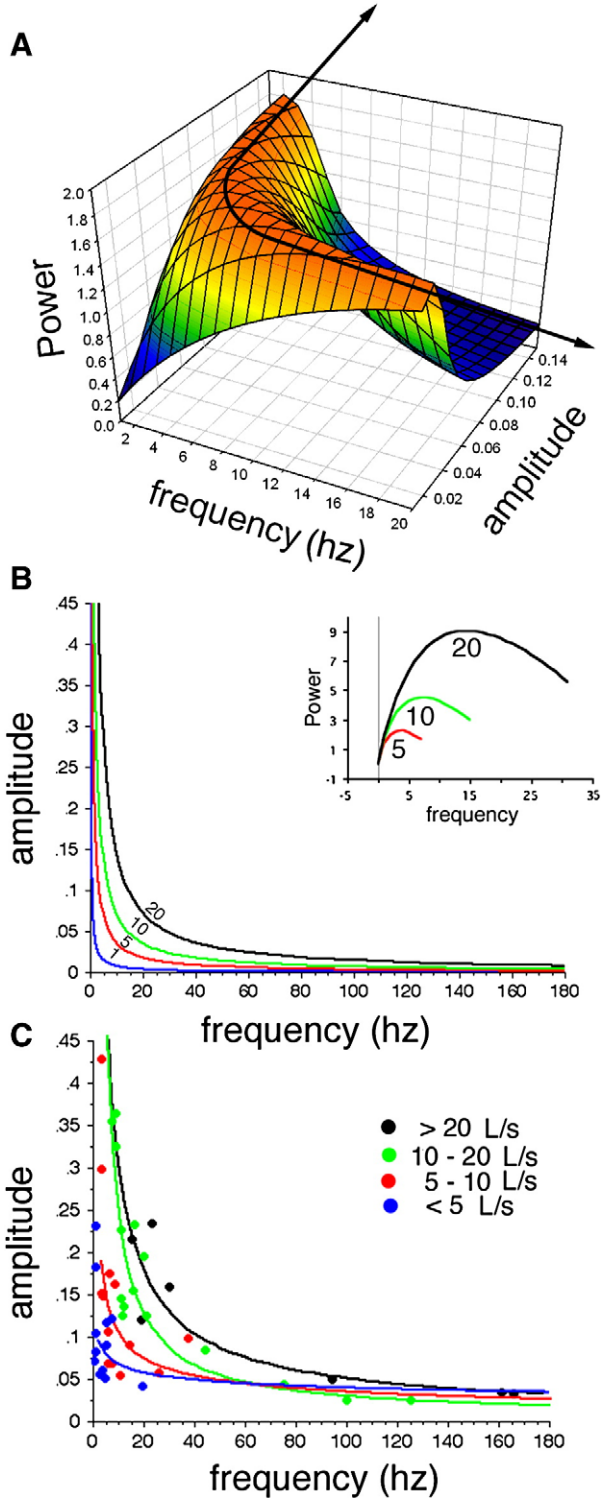

Fig. 2. Sustained muscle power output as a function of both operational frequency (Hz) and strain amplitude (total strain). A. Three dimensional surface plot of sustained power output for a muscle with a V_{max} of 5 lengths/s. Power output is seen as a convex surface, where peak sustained power output is seen as a ridge running nearly parallel to the amplitude axis at low frequencies and turning to run nearly parallel to the frequency axis at low amplitudes. The line along the ridge demarcates the position of peak power output continuing past the range of the graph, with arrows indicating the continued direction of peak power output with respect to both frequency and amplitude. B. Peak power output as a function of frequency and amplitude, with separate lines for different V_{max} (L/s) indicated by numbers on lines. In each case, the shape of the function is similar, while the elevation is proportional to shortening velocity. Plotting these lines on log-transformed axes produces parallel lines with a slope of −1, and an elevation directly proportional to V_{max} (not shown). The inset shows sustained power curves as a function of operational frequency (constant strain amplitude) showing that power output in faster muscles overlaps that of slower muscles. These curves are analogous to instantaneous power curves as a function of shortening velocity. C. Results from a meta-analysis of data from diverse muscles split by V_{max} (blue: <5 L/s; red: 5–10 L/s; green: 10–20 L/s; and black: >20 L/s). Individual subgroups of data were fitted with power curves and the pattern exhibited by these data closely conforms to that predicted in B.

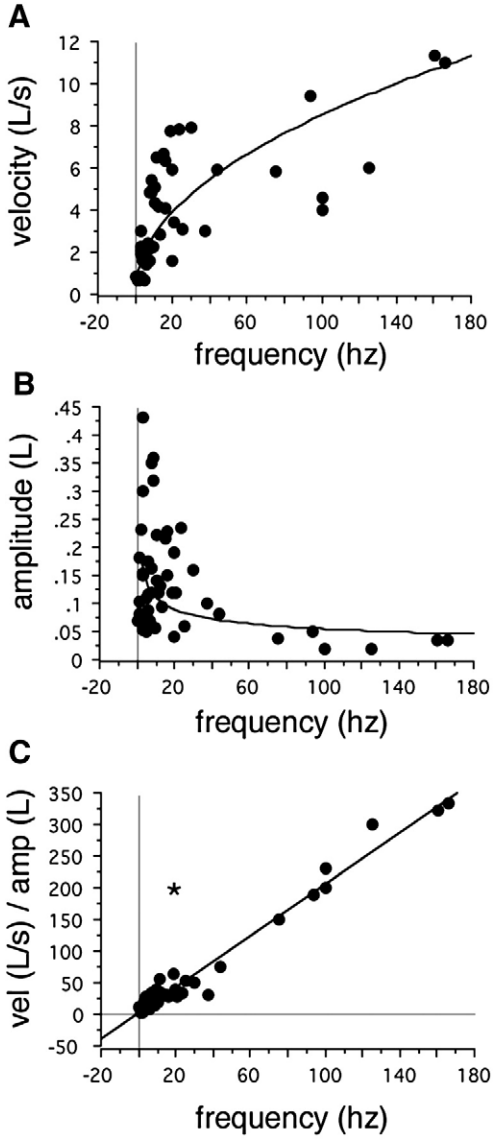

Fig. 3. Interactions among operational frequency, muscle shortening velocity, and strain amplitude. A. A significant correlation exists between muscle shortening velocity and operational frequency (velocity = 0.93 * frequency^{48}; $p<0.0001$). Although muscles with higher operational frequencies tend to be faster, the correlation is non-linear. B. A significant inverse relationship exists between total muscle strain amplitude and operational frequency (amplitude = 0.22 * frequency$^{-0.31}$; $p<0.0001$), but again the relationship is non-linear. These data are the same as those shown in Fig. 2C, but fitted here with a single power regression through all of the data. At frequencies above about 50 Hz, the total muscle shortening is consistently 5% or less. C. A direct linear correlation exists between the *ratio* of muscle shortening velocity and strain amplitude as a function of operational frequency (velocity/amplitude = 2.65 + 2.0 * frequency; $p<0.0001$; $r^2=0.97$). This pattern conforms to the simple relationship: velocity/strain amplitude = 2 * frequency (Eq. (5)). The asterisk indicates where the toadfish swimbladder muscle fits in this relationship. This is a high frequency muscle, capable of producing power at up to 200 Hz, but the frequency where power output is maximum is only 22 Hz. Because of this anomaly, this point was omitted from the regression.

Rearranging the general pattern shown in Fig. 2 yields the systematic relationship:

$$\text{frequency} \propto V_{max} \bullet \text{strain amplitude}^{-1} \quad (4)$$

More precisely, for a muscle undergoing linear ("sawtooth") cycles of shortening and lengthening, the ratio of operational velocity to strain amplitude is equal to twice the frequency:

$$2*\text{frequency} = \text{velocity}*\text{strain amplitude}^{-1} \quad (5)$$

A factor of two is needed here, because for a complete contractile cycle the muscle must both shorten and lengthen over its entire strain amplitude (ie, muscle shortening occurs over one *half* of a total cycle, while muscle lengthening takes place during the other half cycle). The experimental data from diverse muscles (Table 1) closely conformed to this general pattern (Fig. 3C; velocity* strain^{-1} = 2.65 + 2.0* frequency; $r^2=0.97$; $p<0.0001$), where the velocity term in this relationship is the actual operating velocity, rather than the V_{max}. Assuming that muscles operate at a velocity near that which produces maximal power output, then the ratio of V_{max} to amplitude must be proportional to frequency (Eq. (4)).

We also explored how V_{max} and strain amplitude might be tuned to make subtle changes in power output (Fig. 4). The sustained power curve for a given muscle could be shifted by changing the strain amplitude (Fig. 4A), or through modulation of operational frequency (Fig. 4B). In either case, higher operational frequencies could be

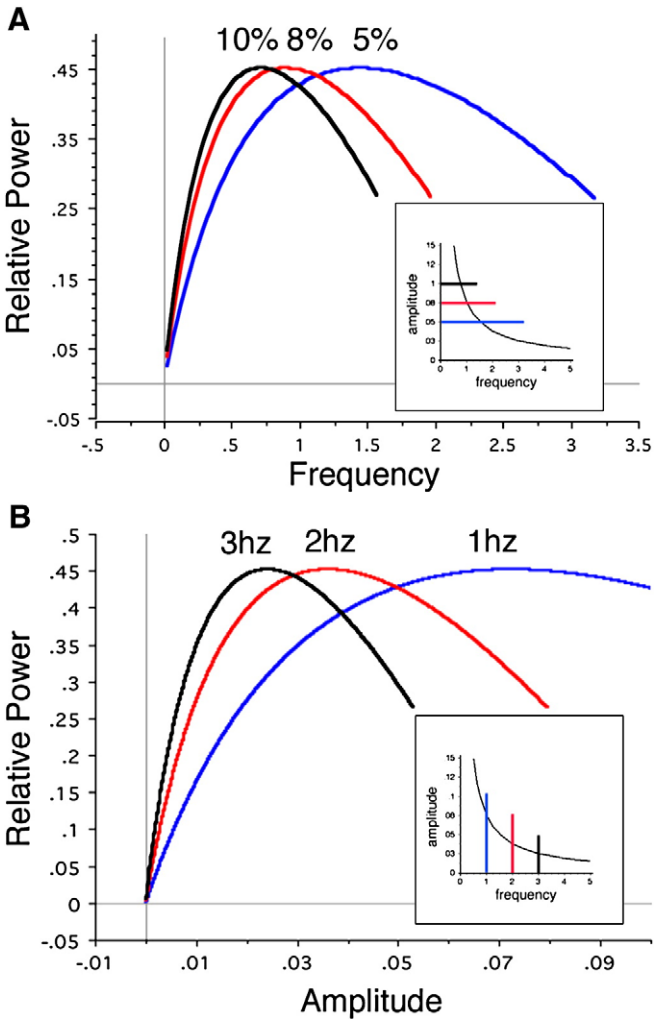

Fig. 4. Relative power output as a function of frequency and strain amplitude for a muscle with a V_{max} of 1 L/s. A. Power output as a function of operational frequency can be modulated by subtle changes in strain amplitude. As strain amplitude becomes greater, the optimal operational frequency decreases and becomes compressed into a sharper peak, but at lower strain amplitudes power output is less sensitive to changes in frequency. B. Power output as a function of stain amplitude can be modulated by adjusting the operational frequency. As muscles operate at higher frequencies, the optimal operational amplitude decreases and becomes compressed into a sharper peak. At lower frequencies, the power output is less sensitive to changes in strain amplitude. The curves in A can be visualized by making three parallel sections through the power surface shown in 2A along the frequency axis, but at different strain amplitudes (A inset). Similarly, the curves in B can be visualized by making three parallel sections along the amplitude axis, but at different frequencies (B inset).

attained by adopting smaller strain amplitudes during cyclical muscle contractions. By contrast, adjusting the muscle force changed the amplitude of power output, but did not shift the shape of the power curve with respect to either frequency or amplitude (data not shown).

3.2. Estimation of human muscle power output

In a case study, we used published values for V_{max} for human muscle fiber types to estimate the frequencies corresponding to maximum power output for each fiber type (Fig. 5). For the slow type I fibers we estimated that power was maximized at 1.5 Hz; for the fast type IIA fibers we found that power output was maximum at 3.7 Hz; and for the fastest, type IIX fiber maximum power was reached at 11 Hz. A general pattern illustrated from our results was that muscles with a higher V_{max} could produce power over a wider range of frequencies than slower muscles (Fig. 5). At the frequency approximate to maximum human stride frequency (~2.5 Hz), the estimated power production from the type IIA fibers was 95% of maximum, from the type I fibers was 82% of maximum, and that from the type IIX fibers was 54% of maximum.

3.3. Scaling effects in mammalian muscles

To predict the change in V_{max} as a function of body size, we used the stride frequency data for mammals reported by Heglund et al. (1974). In one simulation, we fixed strain amplitude and found the V_{max} that maximized power output at the given frequency. In another, we fixed V_{max} and allowed strain amplitude to vary. When strain amplitude was held constant, we found that V_{max} scaled as mass$^{-0.12}$ (Fig. 6), which closely fits previously reported values (Medler, 2002). This scaling exponent is independent of strain amplitude, so long as the strain is the same among different sized mammals. As with the simulation of human muscle fiber types, a general pattern demonstrated here was that faster muscles have the capability to generate power over a wider range of frequencies than slower muscles (Fig. 6B).

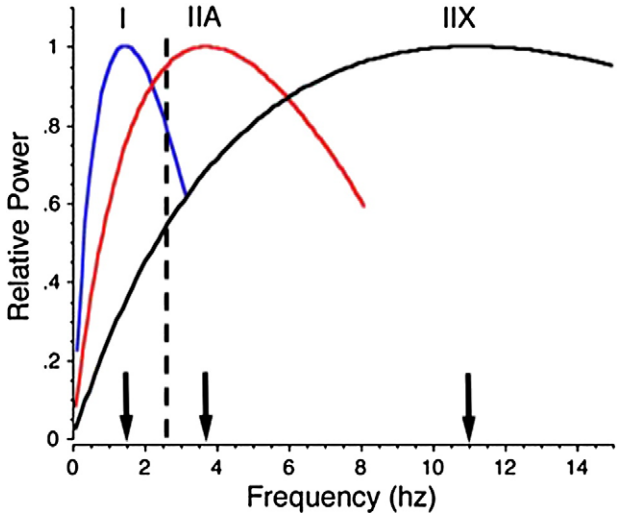

Fig. 5. Relative power output for human muscle fiber types (I, IIA, IIX) at a constant strain (8% total strain). Peak power output is produced at 1.5 Hz for the slow (type I) muscles, 3.7 Hz for the fast (type IIA) muscles, and 11 Hz for the fastest (type IIX) muscles (arrows indicate frequencies corresponding to maximum power output). Power output could be modulated by changes in the strain amplitude, with smaller amplitudes allowing operation at higher frequencies (see Fig. 4A). These data illustrate the need to recruit faster muscles as stride frequency increases during running. At lower walking or running speeds, type I and IIA fibers are probably sufficient to power movement. As running speed increases, it will be necessary to shift toward the type IIA and IIX muscle fibers to effectively produce power output as stride frequency increases. The vertical dashed line indicates the frequency limits of human performance based on maximal stride frequencies during running, and pedaling frequencies generating maximal power during cycling. This frequency limit (~2.5 Hz) is in the range intermediate between the type I and type IIA fibers that are predominant in human leg muscles.

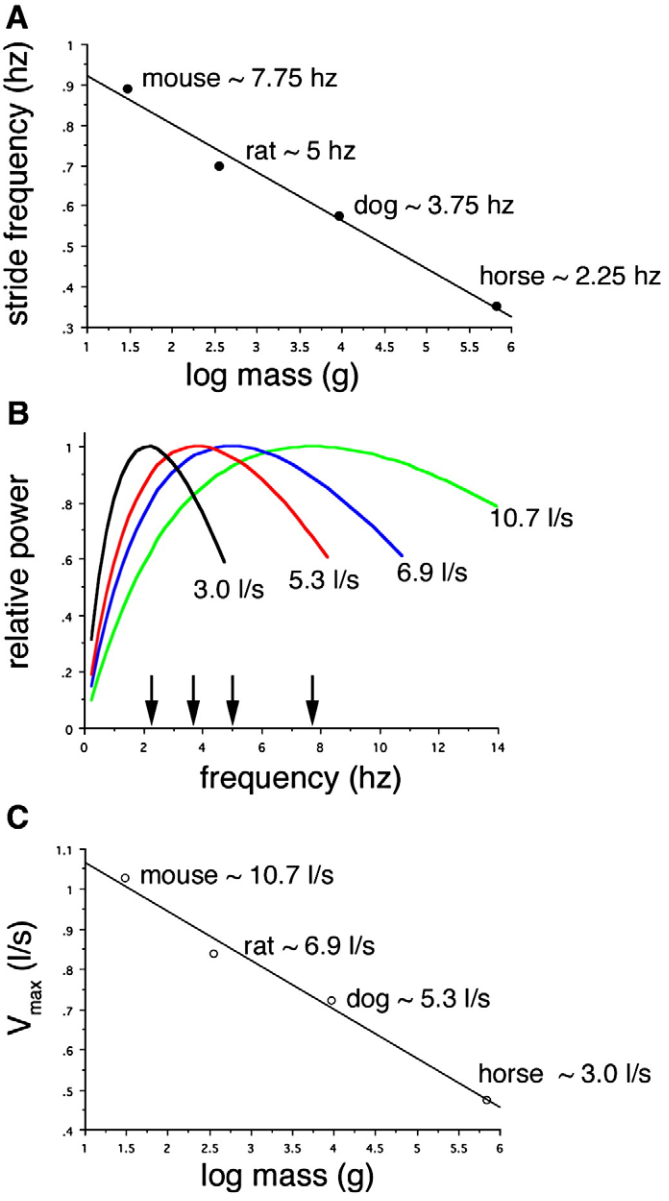

Fig. 6. Scaling effects on operational frequency and muscle power output. A. Relationship between stride frequency (log scale) at the trot to gallop transition for the mammals shown in Fig. 1 of Heglund et al. (1974). Stride frequency is proportional to mass$^{-0.12}$. B. Model results of individual power curves generated to maximize power at the frequencies corresponding to stride frequencies in A. Total strain amplitudes were fixed at 10% of muscle length. Muscle shortening velocities (L/s) are indicated for each curve, and frequencies corresponding to maximal relative power output are indicated by arrows. C. Muscle shortening velocities (log scale) estimated in B are plotted as a function of body mass. As with stride frequency, the optimal V_{max} scales as mass$^{-0.12}$.

4. Discussion

4.1. Muscle design, constraints, and power output

Skeletal muscles operating in diverse animals exhibit a wide array of specific contractile capabilities. This variability in physiological function is derived from a number of muscle design parameters, as well as specific design constraints. Design parameters are those muscle properties that can be adjusted to affect muscle function and include factors such as shortening velocity, metabolic capacity, and the kinetics of muscle activation and deactivation (Rome and Lindstedt, 1997).

Design constraints represent the boundaries of muscle organization that ultimately limit the physiological capabilities of skeletal muscles. Well-known design constraints include the force-length characteristics of muscles, instantaneous power output being achieved at approximately 30% of V_{max}, and the amount of force produced per cross-sectional muscle area (Rome and Lindstedt, 1997). In this context, we report a systematic design constraint in the relationships among operational frequency, strain amplitude, and V_{max}. Muscle shortening velocity during cyclical contractions is proportional to the product of contractile frequency and strain amplitude (Eqs. (4) and (5)). Consistent with this, our model predicts that power output is maximized along a line where the product of frequency and strain amplitude are constant (Eq. (4) and Fig. 2). The precise elevation of each line is determined by the V_{max}, with faster muscles being shifted upward and to the right on the frequency–amplitude graph (Fig. 2B and C). Assuming that muscles operate with a shortening velocity close to that which generates maximum power output, one may view these "iso-velocity curves" (Fig. 2B) as representing the ratio of cycle frequency to muscle strain that generates this optimal shortening velocity for a particular V_{max}. This simple relationship is a basic manifestation of the force–velocity relationship that arises during cyclical muscle contraction, and it has a number of important implications for understanding muscle function.

Isolated muscles performing oscillatory contractions maximize power at an optimal frequency (Altringham and Young, 1991; Johnson et al., 1993; Swoap et al., 1993; Askew and Marsh, 1997; Josephson, 1997; Swoap et al., 1997; Harwood et al., 1998; Shiels et al., 1998; Josephson et al., 2000b; Syme and Shadwick, 2002). A similar pattern is exhibited for power output from human cyclists, where the relationship between power output and cycle frequency appears to stem directly from the force–velocity properties of the skeletal muscles (Minetti et al., 1995; MacIntosh et al., 2000; Martin, 2007; Sargeant, 2007). Other reviews have also emphasized the central role of the force–velocity relationship with respect to contractile frequency and power output, but they do not address the importance of strain amplitude in their discussions (Martin, 2007; Sargeant, 2007). Amplitude must be taken into account, because either V_{max} or strain amplitude may be adjusted to maximize power output. Given that either of these parameters can determine optimal frequency, it becomes important to consider what conditions might favor V_{max} versus strain amplitude as the primary parameter determining operational frequency.

One factor that influences the degree to which V_{max} and strain amplitude interact to set the operational frequency is the anatomical organization, or architecture, of the muscle (Lieber, 1992; Lieber and Friden, 2000). This is because the muscle architectural arrangement and the position of muscle insertion determine the muscle's gear ratio, which is the relative degree of joint movement produced for a given amount of muscle shortening (Rome et al., 1988; Rome and Lindstedt, 1997). A muscle's gear ratio represents another important design parameter in musculoskeletal systems, and for effective operation during locomotion it is essential that a muscle's V_{max} be appropriately matched with the muscle's gear ratio (Rome et al., 1988). Likewise, it is important that the muscle's strain amplitude be effectively coupled to its gear ratio. This is particularly true for muscles operating with minimal levels of shortening, since some mechanism must exist to amplify the muscle shortening into mechanically relevant movements. A dramatic example of this is the production of wing movement observed in certain orders of insects that use asynchronous muscles for flight, where the flight muscles are not attached to the wings, but to an elastic thorax that acts as a mechanical oscillator (Dickinson and Tu, 1997; Josephson, 1997; Dickinson, 2006). These muscles are able to operate with high frequencies, in spite of the fact that their intrinsic V_{max} is not remarkably high, because they contract with very small strain amplitudes and the thorax and wings amplify the movements.

A second factor influencing the interplay between V_{max} and strain amplitude is the upper ceiling of muscle shortening velocity. Maximum muscle shortening velocities are limited to approximately 25 lengths/s, even in muscles that operate at high frequencies (Josephson, 1993; Medler, 2002). This is likely a consequence of the design constraints resulting from the molecular organization of the myosin heavy chain motor that is responsible for all muscle contraction. Comparative studies reveal that although most of the structure of the molecule is highly conserved among species, subtle alterations of the loop 1 and loop 2 regions of the molecule (surface loops near the ATP- and actin-binding regions, respectively) result in significant changes in contractile kinetics (Reggiani et al., 2000; Pellegrino et al., 2003). However, the upper limits to how fast a muscle can contract mean that at higher operational frequencies, V_{max} cannot increase proportionally and strain amplitude must decline to produce power. Muscles that contract at ~50 Hz or above consistently operate with minimal shortening (Figs. 2C and 3B).

4.2. Implications for performance limitations

One of the useful applications of our model is for predicting the range of operational frequencies available to a muscle based on its mechanical properties measured *in vitro*. Alternatively, kinematic analyses of moving animals can be used to predict the kinetic properties of isolated muscles. As an example of this, we focused on modeling the power output from different human muscle fibers (I, IIA, and IIX) and interpreted out results within the context of athletic performance. The speed of locomotion depends directly on the frequency of movement of the appendages, or more precisely, maximum running speed is a function of both stride length and frequency (Hunter et al., 2004; Ahlborn et al., 2006). Our results suggest that the maximum cycle frequency may set upper limits to locomotory speed, which is ultimately determined by the V_{max} of the muscle. As an example of this, we modeled the power output from simulated human muscles (type I, IIA, or IIX) at a range of operating frequencies. The results indicate that the optimal operational frequencies for these muscles are approximately 1.5 Hz, 3.67 Hz, and 11 Hz for the different fiber types (Fig. 5). It is interesting that the maximal stride frequency in trained sprinters and cyclists of approximately 2–2.5 Hz (Hunter et al., 2004; Sargeant, 2007) is intermediate between the optimal frequencies predicted for type I and IIA muscle fibers (Fig. 5). The type I and IIA fibers are the prevalent types in human leg muscles (type IIX fibers generally represent less than 10% of the fibers (Andersen and Aagaard, 2000; Williamson et al., 2001a; Parcell et al., 2003; Kohn et al., 2007)), and the frequency-dependence of human muscle power output is directly linked to the expressed MHC isoforms in a muscle (McCartney et al., 1983; Pearson et al., 2006; Sargeant, 2007). This pattern suggests that maximal running speed may be constrained by the ability to generate power output at higher frequencies. In this context, it has been reported that top running speed in lizards is not limited by muscle power output, since lizards running uphill can generate greater power than that produced at top speed (Farley, 1997). We contend that the issue of muscle power output must be discussed in the context of stride frequency. It is not power output *per se*, but power output at a particular frequency, that likely limits top running speed. At sub-maximal operating frequencies, it will be possible to increase power output by increasing muscle mass (force), but this will not translate into faster running speeds if stride frequency ultimately limits top speed.

4.3. Resonance in locomotion

One of the most important implications for our results is related to the integrative aspects of animal locomotion. Diverse animals operating with different modes of locomotion take advantage of spring-like properties in their musculoskeletal systems to minimize the active energy requirements from their skeletal muscles (Farley et al., 1993; Pabst, 1996; Biewener, 2006). One outcome of these spring-like properties is that many animals possess resonant properties in their musculoskeletal systems, which means that efficient movement is dependent on operational frequency (Greenwalt, 1960; Turvey et al., 1988; Holt et al., 1990; Ahlborn and Blake, 2002; Ahlborn et al., 2006).

Ahlborn et al. (2006) provide a compelling discussion of the importance of these resonant properties in animal locomotion and discuss some of the mechanisms available to effectively tune the resonant frequency to the frequency of operation. In an earlier study, they demonstrated that the energy required to drive a system takes a sharp drop as the resonant frequency is approached (Ahlborn and Blake, 2002). In fact, driving a system at twice its resonant frequency is predicted to require *15 times* the power than for the same system operating at resonance (Ahlborn and Blake, 2002). Clearly, for a skeletal muscle to drive an oscillating system efficiently it must be able to produce power at or near the resonant frequency of the whole system. One of the most compelling examples of this coupling is from the asynchronous muscles of insect flight muscles, where normal operation is dependent on coupling of the power-generating muscles to an appropriate oscillating load (Josephson et al., 2000a; Dickinson, 2006).

Experimental data from isolated muscles support the idea that muscles generate maximum power output at or near the same frequency operating *in vivo* (Altringham and Young, 1991; Johnson et al., 1993; Swoap et al., 1993; Josephson, 1997; Harwood et al., 1998; Shiels et al., 1998; Syme and Shadwick, 2002) and animals adopt a movement frequency near resonance (Greenwalt, 1960; Alexander, 2000; Ahlborn and Blake, 2002; Ahlborn et al., 2006). Therefore, the resonant properties of biomechanical systems used for locomotion appear to be co-adapted with the active power generating properties of the skeletal muscles. In this context, it is interesting to note that faster muscles can generate optimal power over a wider range of operating frequencies (Fig. 2B inset, 5, and 6B). This pattern has important implications for how the kinetic properties of muscles have co-evolved with the resonant properties of the musculoskeletal system as a whole. Further research is needed to integrate the active kinetic properties of muscles, and the underlying cellular and molecular organization responsible for these, with the biomechanical aspects of the musculoskeletal system (*see 4.5. Muscle plasticity and hybrid muscle fibers*).

Another important question is whether the resonant properties of the musculoskeletal system and the frequency dependence of power production can be altered dynamically. Within limits, the passive resonant properties of animals exhibited during processes of locomotion can be effectively adjusted, or tuned, to meet the energetic needs of the animal. Examples of this is tuning include the dynamic changes in limb stiffness, as well as changes in this geometry of joints used during movement (Ahlborn et al., 2006). Likewise, cyclically contracting skeletal muscles have some capability to adjust their power output as the conditions demand. The most obvious example of this process is the sequential recruitment of different motor units (Wakeling, 2005). At slower running speeds, smaller units comprised of slower skeletal muscles may be appropriate, but as running speed increases the faster muscles must become active to produce power at higher frequencies (Fig. 5).

Moreover, our model predicts that effective tuning of power output can be accomplished through rather subtle changes in operational frequency, strain amplitude, or a combination of the two (Fig. 4). The patterns shown in Fig. 4 are highly consistent with experimental data for isolated muscles, which demonstrate that at higher operational frequencies, the strain amplitude required to maintain power output becomes compressed to lower amplitudes (Swoap et al., 1997; Josephson et al., 2000b). Furthermore, studies of motor behavior also report dynamic shifts in joint stiffness to adjust to different operational frequencies (Hatsopoulos and Warren, 1996; Abe and Yamada, 2003). In principle, it should be possible for animals to dynamically adjust the resonant properties of their bodies, along with the power generating capacity of their skeletal muscles, to optimize the coupling between these systems.

4.4. Scale effects on skeletal muscle design

One of the clearest examples of the coupling between muscle kinetics and passive resonant properties comes from the effect of body size, or scale, on skeletal muscle biology. Hill recognized that the physical dimensions of animals' bodies affect the contractile properties of their skeletal muscles, with smaller animals generally possessing faster contracting muscles than larger species (Hill, 1950). McMahon later refined this hypothesis, using the effects of body size to explore the design of locomotory systems in animals (McMahon, 1975). He demonstrated that mechanical systems used for locomotion have natural frequencies of operation that can be determined by simply considering the physical dimensions of limbs and joints (McMahon, 1975). In his analyses, McMahon made two critical assumptions. First, he assumed that the contractile properties of the skeletal muscles should be matched to the natural frequency of the operating system. This is essentially the same principle we are proposing in the preceding discussion, as scale effects represent a special case of resonance in locomotion. Second, he assumed that the V_{max} of the skeletal muscle should determine the frequency of operation. If we ignore the impact of strain amplitude in our analysis and assume that muscles from similar species operate using the same amount of muscle shortening, then V_{max} and frequency are directly correlated. When we optimized muscle V_{max} in our model to maximize power output at the frequency of running for different sized terrestrial mammals (Heglund et al., 1974), we found that V_{max} scaled as mass$^{-0.12}$ (Fig. 6), similar to the general pattern known for running and flying animals (Lindstedt et al., 1985; Medler, 2002). This mass exponent also matches theoretically derived and empirically observed mass exponents for running and flying animals' operational frequencies (Heglund et al., 1974; Turvey et al., 1988; Calder, 1996; Full, 1997). The close correlation between the allometry of operational frequency and optimal muscle contractile frequency supports the hypothesis that the power generating properties of muscles are closely matched to the resonant properties of the musculoskeletal system.

The effects of scale on the resonant properties of the musculoskeletal system influence skeletal muscle design in two related ways. From an evolutionary standpoint, muscles should be shaped by selective pressure to possess kinetic properties closely matched to the kinetic properties attributable to the physical characteristics of the skeleton and other connective tissues (Alexander, 2000). There is substantial evidence that muscles of many types have, in fact, been shaped by this coupling. Muscles from diverse animals all conform to the same general scaling relationship, where the V_{max} declines as a predictable function of body mass (Lindstedt et al., 1985; Reggiani et al., 2000; Medler, 2002; Marx et al., 2006). Consistent with this, orthologous MHC isoforms exhibit subtle differences in their molecular organization that are at least partially responsible for these differences in V_{max} (Reggiani et al., 2000). In this context, it is interesting that the fastest (2B) MHC isoform has become a pseudogene in larger mammals and is no longer functional (Chikuni et al., 2004). We conclude that the effective loss of this fastest MHC isoform can be explained by the fact that as these species evolved to larger sizes, this fastest isoform no longer matched the resonant operating frequencies used during locomotion.

A second effect of body size is related to ontogenetic effects for animals that significantly increase in size over their lifetime. Many animals increase in mass by several orders of magnitude over a lifetime, and the resonant properties of their limbs change throughout their lifetimes, as the relative proportion of the limbs change. From the standpoint of muscle plasticity, muscles are anticipated to continually alter their phenotype as the animal grows, meaning that the muscles should become slower as the resonant operating frequency decreases. In fact, this process is clearly evident for muscles used in terrestrial running and for swimming (see data for *Dipsosaurus dorsalis* and *Gadus morhua* in Table 1). Isolated muscles from a number of species exhibit systematic shifts in muscle kinetics as the animals grow larger (Marsh, 1988; Altringham and Johnston, 1990; Anderson and Johnston, 1992; Johnson et al., 1993; James et al., 1998; James and Johnston, 1998; Van Wassenbergh et al., 2007). Thus far, the cellular and molecular mechanisms responsible for these changes have not been identified, but one likely possibility is a shift in the expression of the specific MHC isoforms.

4.5. Muscle plasticity and hybrid muscle fibers

Skeletal muscles are highly plastic tissues, capable of remodeling their cellular and molecular properties in response to a variety of demands (Schiaffino and Reggiani, 1996; Caiozzo, 2002; Pette, 2002). This plasticity is directly relevant to the ability of skeletal muscles to provide power during cyclical muscle contractions, since changes in myofibrillar isoforms in the muscle fibers directly affect their mechanical capabilities (Caiozzo, 2002).

The most obvious mechanism available to tune the active contractile properties of skeletal muscles is through the expression of different myosin heavy chain (MHC) isoforms. In mammalian muscles, MHC isoforms are encoded by several different genes (Schiaffino and Reggiani, 1996), while in *Drosophila* (and presumably other animals) alternative splicing of a single MHC gene yields different isoforms (Emerson and Bernstein, 1987). The force–velocity properties of muscles are, to a large extent, the direct result of the MHC isoforms operating in the muscle (Schiaffino and Reggiani, 1996; Caiozzo, 2002). Animals generally possess multiple isoforms of MHC spanning about a 10-fold range of shortening velocities, which provide effective shortening speeds for a variety of different movements. The MHC expression in a muscle is not fixed, but changes dynamically in response to a variety of external stimuli (Schiaffino and Reggiani, 1996; Caiozzo, 2002). In recent years, it has become increasingly clear that many single fibers possess two or more different MHC isoforms (Stephenson, 2001; Caiozzo et al., 2003; Medler et al., 2004). These 'hybrid' muscle fibers possess force–velocity properties intermediate to 'pure' muscle fiber types, and the context of the current discussion, it seems likely that subtle changes in the active contractile properties of muscles can be achieved by changing the expression of different MHC isoforms. Caiozzo et al. (2003) noted that the polymorphism exhibited by many muscle fibers provides the potential for a continuum of fiber types, defined by the relative proportion of MHC isoforms present in the muscle fibers.

In addition to MHC expression, changes in other myofibrillar genes might be important for making adjustments in operational frequency. Among these, certain myosin light chain (MLC) isoforms are known to influence the force–velocity properties of muscles (Schiaffino and Reggiani, 1996). Furthermore, phosphorylation of the regulatory myosin light chain has the potential to affect muscle force–velocity properties dynamically (Grange et al., 1993; Davis et al., 2002; MacIntosh and Bryan, 2002). Further research is clearly needed to determine the mechanisms that might be employed to dynamically tune the mechanical properties of skeletal muscles.

4.6. Muscle activation, deactivation, and other complexities

Finally, our results emphasize the importance of the force–velocity relationship in determining the central tendency of cyclically contracting muscles to produce sustained power at a specific strain amplitude/frequency ratio. However, patterns of muscle power output *in vivo* are complex and do not relate exclusively to the force–velocity properties of a muscle, but are influenced by a number of parameters. For example, muscle activation, deactivation, force–length properties, and other factors also significantly impact muscle power output (Marsh, 1990; Josephson, 1999; Marsh, 1999; Caiozzo, 2002). Muscle deactivation in particular seems to have an important role in limiting contractile frequency in muscles (Marsh, 1990). In our model, we selectively omitted these parameters by modeling muscle activation and deactivation as instantaneous, and muscle length as optimal for force production. What we present, therefore, is an upper ceiling of power output and should be viewed as a central tendency for the conditions required to maximize power output (Caiozzo, 2002). In real-world muscles, power production will be shifted downward because of power lost to activation, deactivation, or changes in muscle length. Activation and deactivation limitations become increasingly important at higher frequencies, as the relative proportion of each cycle occupied by activation and deactivation events becomes greater (Caiozzo and Baldwin, 1997; Martin, 2007). Another factor we have not accounted for is the effect of pre-stretch of the muscle before activation. Pre-stretch may enhance power output, because the forces produced during muscle lengthening are significantly greater than those produced during muscle shortening (Josephson, 1993; Josephson, 1999). Therefore, eccentric muscle contraction immediately preceding muscle shortening may increase the muscle force at the beginning of a contraction cycle and increase sustained power output. Each of these muscle parameters may have the effect to shift the sustained power production during cyclical contractions, but are not required to explain the fundamental frequency dependence of power generation by skeletal muscles. The central effects of the force–velocity properties of the muscle clearly constrain the frequency of muscle contraction and represent a primary determinant of sustained power output.

5. Conclusions

In summary, cyclically contracting muscles generate the power required to drive a diversity of physiological processes. Using a simple model of sustained power output for muscles operating over a range of frequencies, we have identified a number of important trends directly relevant to our understanding of skeletal muscle design. These include the following principles:

- A basic design constraint exists among the intrinsic shortening velocity, strain amplitude, and frequency of operation of a muscle. Specifically, optimal power output is proportional to the *ratio* of shortening velocity and strain amplitude and either of these parameters may be adjusted to match a specific frequency of operation.
- Power output displays a parabolic relationship as a function of operational frequency, with each muscle fiber type possessing a limited range of frequencies that maximize power output.
- Absolute power output can be modulated by changing the force of the muscle (ie., through cross sectional area), but this does not shift the optimal frequency of the muscle. To shift the optimal frequency, the force–velocity properties of the muscle must change (ie., through fiber type).
- The width of the power curve as a function of frequency is positively correlated with muscle shortening velocity, with faster muscles having the potential to generate power over a wider range of frequencies.
- For muscles operating at high frequencies, the strain amplitude must be small and the range of effective operational frequencies is narrow.
- The above principles have important implications for resonance in locomotion, where the mechanical properties of the musculoskeletal system limit the range of effective operational frequencies. Specifically, our results predict that the optimal contractile frequency of muscles driving the system will be tuned to match the natural frequency attributable to the physical properties of the skeleton and other connective tissues.

Diverse skeletal muscles employ a wide range of operating parameters to carry out their specific functions (Table 1), yet the basic mechanism of muscle contraction is conserved. Each of the above principles helps to explain the diversity of functional parameters and has potentially important implications for understanding broad patterns of muscle design and function.

Acknowledgments

This work was supported by an Interdisciplinary Research Development Fund (IRDF) grant at the University of Buffalo. We also appreciate editorial suggestions from Dr. Scott C. White and two anonymous reviewers.

References

Abe, M.O., Yamada, N., 2003. Modulation of elbow stiffness in a vertical plane during cyclic movement at lower or higher frequencies than natural frequency. Exp. Brain Res. 153, 394–399.

Ahlborn, B.K., Blake, R.W., 2002. Walking and running at resonance. Zoology 105, 165–174.

Ahlborn, B.K., Blake, R.W., Megill, W.M., 2006. Frequency tuning in animal locomotion. Zoology 109, 43–53.

Alexander, R.M., 2000. Optimization of muscles and movement for performance or economy of energy. Neth. J. Zool. 50, 101–112.

Altringham, J.D., Johnston, I.A., 1990. Scaling effects on muscle function: power output of isolated fish muscle fibres performing oscillatory work. J. Exp. Biol. 151, 453–467.

Altringham, J.D., Young, I.S., 1991. Power output and the frequency of oscillatory work in mammalian diaphragm muscle: the effects of animal size. J. Exp. Biol. 157, 381–389.

Andersen, J.L., Aagaard, P., 2000. Myosin heavy chain IIx overshoot in human skeletal muscle. Muscle Nerve 23, 1095–1104.

Anderson, M.E., Johnston, I.A., 1992. Scaling of power output in fast muscle-fibers of the atlantic cod during cyclical contractions. J. Exp. Biol. 170, 143–154.

Askew, G.N., Marsh, R.L., 1997. The effects of length trajectory on the mechanical power output of mouse skeletal muscle. J. Exp. Biol. 200, 3119–3131.

Askew, G.N., Marsh, R.L., 1998. Optimal shortening velocity (V/V-max) of skeletal muscle during cyclical contractions: Length–force effects and velocity-dependent activation and deactivation. J. Exp. Biol. 201, 1527–1540.

Askew, G.N., Marsh, R.L., 2001. The mechanical power output of the pectoralis muscle of blue-breasted quail (Coturnix chinensis): the in vivo length cycle and its implications for muscle performance. J. Exp. Biol. 204, 3587–3600.

Bennet-Clark, H.C., Daws, A.G., 1999. Transduction of mechanical energy into sound energy in the cicada Cyclochila australasiae. J. Exp. Biol. 202, 1803–1817.

Biewener, A.A., 2006. Patterns of mechanical energy change in tetrapod gait: pendula, springs and work. J. Exp. Zool. 305A, 899–911.

Biewener, A.A., Corning, W.R., Tobalske, B.W., 1998. In vivo pectoralis muscle force-length behavior during level flight in pigeons (Columba livia). J. Exp. Biol. 201, 3293–3307.

Biewener, A.A., Dial, K.P., Goslow, G.E., 1992. Pectoralis muscle force and power output during flight in the starling. J. Exp. Biol. 164, 1–18.

Caiozzo, V.J., 2002. Plasticity of skeletal muscle phenotype: mechanical consequences. Muscle Nerve 26, 740–768.

Caiozzo, V.J., Baldwin, K.M., 1997. Determinants of work produced by skeletal muscle: potential limitations of activation and relaxation. Am. J. Physiol. Cell. Physiol. 42, C1049–C1056.

Caiozzo, V.J., Baker, M.J., Huang, K., Chou, H., Wu, Y.Z., Baldwin, K.M., 2003. Single-fiber myosin heavy chain polymorphism: how many patterns and what proportions? Am. J. Physiol. Regul. Integr. Comp. Physiol. 285, R570–R580.

Calder, W.A., 1996. Size, Function, and Life History. Harvard University Press, Cambridge, Mass.

Carrier, D.R., Gregersen, C.S., Silverton, N.A., 1998. Dynamic gearing in running dogs. J. Exp. Biol. 201, 3185–3195.

Chan, W.P., Dickinson, M.H., 1996. In vivo length oscillations of indirect flight muscles in the fruit fly Drosophila virilis. J. Exp. Biol. 199, 2767–2774.

Chikuni, K., Muroya, S., Nakajima, I., 2004. Absence of the functional myosin heavy chain 2b isoform in equine skeletal muscles. Zool. Sci. 21, 589–596.

Coughlin, D.J., Zhang, G.X., Rome, L.C., 1996. Contraction dynamics and power production of pink muscle of the scup (Stenotomus chrysops). J. Exp. Biol. 199, 2703–2712.

Daniel, T.L., Tu, M.S., 1999. Animal movement, mechanical tuning and coupled systems. J. Exp. Biol. 202, 3415–3421.

Davis, J.S., Satorius, C.L., Epstein, N.D., 2002. Kinetic effects of myosin regulatory light chain phosphorylation on skeletal muscle contraction. Biophys. J. 83, 359–370.

Dickinson, M., 2006. Insect flight. Curr. Biol. 16, R309–R314.

Dickinson, M.H., Tu, M.S., 1997. The function of dipteran flight muscle. Comp. Biochem. Physiol. A 116, 223–238.

Dickinson, M.H., Farley, C.T., Full, R.J., Koehl, M.A.R., Kram, R., Lehman, S., 2000. How animals move: an integrative view. Science 288, 100–106.

Ellerby, D.J., Askew, G.N., 2007. Modulation of flight muscle power output in budgerigars Melopsittacus undulatus and zebra finches Taeniopygia guttata: in vitro muscle performance. J. Exp. Biol. 210, 3780–3788.

Emerson, C.P., Bernstein, S.I., 1987. Molecular genetics of myosin. Annu. Rev. Biochem. 56, 695–726.

Farley, C.T., 1997. Maximum speed and mechanical power output in lizards. J. Exp. Biol. 200, 2189–2195.

Farley, C.T., Glasheen, J., McMahon, T.A., 1993. Running springs – speed and animal size. J. Exp. Biol. 185, 71–86.

Fitzhugh, G.H., Marden, J.H., 1997. Maturational changes in troponin T expression Ca2+-sensitivity and twitch contraction kinetics in dragonfly flight muscle. J. Exp. Biol. 200, 1473–1482.

Full, R.J., 1997. Invertebrate locomotor systems. Handbook of Physiology, Section 13. Comparative Physiology, vol. II. American Physiological Society, Bethesda, MD, pp. 853–930.

Full, R.J., Stokes, D.R., Ahn, A.N., Josephson, R.K., 1998. Energy absorption during running by leg muscles in a cockroach. J. Exp. Biol. 201, 997–1012.

Gillis, G.B., Flynn, J.P., McGuigan, P., Biewener, A.A., 2005. Patterns of strain and activation in the thigh muscles of goats across gaits during level locomotion. J. Exp. Biol. 208, 4599–4611.

Girgenrath, M., Marsh, R.L., 1999. Power output of sound-producing muscles in the tree frogs Hyla versicolor and Hyla chrysoscelis. J. Exp. Biol. 202, 3225–3237.

Grange, R.W., Vandenboom, R., Houston, M.E., 1993. Physiological significance of myosin phosphorylation in skeletal muscle. Can. J. Appl. Physiol. 18, 229–242.

Greenwalt, C.H., 1960. The wings of insects and birds as mechanical oscillators. Proc. Am. Phil. Soc, 104, 605–611.

Gregersen, C.S., Silverton, N.A., Carrier, D.R., 1998. External work and potential for elastic storage at the limb joints of running dogs. J. Exp. Biol. 201, 3197–3210.

Harwood, C.L., Young, I.S., Altringham, J.D., 1998. Influence of cycle frequency, muscle strain and muscle length on work and power production of rainbow trout (Oncorhynhcus mykiss) ventricular muscle. J. Exp. Biol. 201, 2723–2733.

Hatsopoulos, N.G., Warren, W.H., 1996. Resonance tuning in rhythmic arm movements. J. Motor Behav. 28, 3–14.

Heglund, N.C., Taylor, C.R., McMahon, T.A., 1974. Scaling stride frequency and gait to animal size – mice to horses. Science 186, 1112–1113.

Hill, A., 1938. The heat of shortening and the dynamic constants of muscle. Proc. R. Soc. Lond. B. Biol. Sci. 38, 209–230.

Hill, A.V., 1950. The dimensions of animals and their muscular dynamics. Sci. Prog. 38, 209–230.

Holmes, P., Full, R.J., Koditschek, D., Guckenheimer, J., 2006. The dynamics of legged locomotion: models, analyses, and challenges. Siam Rev. 48, 207–304.

Holt, K.G., Hamill, J., Andres, R.O., 1990. The force-driven harmonic-oscillator as a model for human locomotion. Hum. Mov. Sci. 9, 55–68.

Hoyt, D.F., Wickler, S.J., Biewener, A.A., Cogger, E.A., De La Paz, K.L., 2005. In vivo muscle function vs speed I. muscle strain in relation to length change of the muscle-tendon unit. J. Exp. Biol. 208, 1175–1190.

Hunter, J.P., Marsh, R.N., McNair, P.J., 2004. Interaction of step length and step rate during sprint running. Med. Sci. Sports Exerc. 36, 261–271.

Ishikawa, M., Pakaslahti, J., Komi, P.V., 2007. Medial gastocnemius muscle behavior during human running and walking. Gait Post 25, 380–384.

James, R.S., Johnston, I.A., 1998. Scaling of muscle performance during escape responses in the fish Myoxocephalus scorpius L. J. Exp. Biol. 201, 913–923.

James, R.S., Altringham, J.D., Goldspink, D.F., 1995. The mechanical properties of fast and slow skeletal muscles of the mouse in relation to their locomotory function. J. Exp. Biol. 198, 491–502.

James, R.S., Cole, N.J., Davies, M.L.F., Johnston, I.A., 1998. Scaling of intrinsic contractile properties and myofibrillar protein composition of fast muscle in the fish Myoxocephalus scorpius L. J. Exp. Biol. 201, 901–912.

Johnson, T.P., Swoap, S.J., Bennett, A.F., Josephson, R.K., 1993. Body size, muscle power output and limitations on burst locomotor performance in the lizard Dipsosaurus dorsalis. J. Exp. Biol. 174, 199–213.

Josephson, R.K., 1985a. Mechanical power output from striated muscle during cyclic contraction. J. Exp. Biol. 114, 493–512.

Josephson, R.K., 1985b. The mechanical power output of a tettigoniid wing muscle during singing and flight. J. Exp. Biol. 117, 357–368.

Josephson, R.K., 1989. Power output from skeletal muscle during linear and sinusoidal shortening. J. Exp. Biol. 147, 533–537.

Josephson, R.K., 1993. Contraction dynamics and power output of skeletal muscle. Annu. Rev. Physiol. 55, 527–546.

Josephson, R.K., 1997. Power output from a flight muscle of the bumblebee Bombus terrestris II. characterization of the parameters affecting power output. J. Exp. Biol. 200, 1227–1239.

Josephson, R.K., 1999. Dissecting muscle power output. J. Exp. Biol. 202, 3369–3375.

Josephson, R.K., Ellington, C.P., 1997. Power output from a flight muscle of the bumblebee Bombus terrestris.1. Some features of the dorso-ventral flight muscle. J. Exp. Biol. 200, 1215–1226.

Josephson, R.K., Stokes, D.R., 1994. Contractile properties of a high-frequency muscle from a crustacean. 3. mechanical power output. J. Exp. Biol. 187, 295–303.

Josephson, R.K., Malamud, J.G., Stokes, D.R., 2000a. Asynchronous muscle: a primer. J. Exp. Biol. 203, 2713–2722.

Josephson, R.K., Malamud, J.G., Stokes, D.R., 2000b. Power output by an asynchronous flight muscle from a beetle. J. Exp. Biol. 203, 2667–2689.

Kernighan, B.W., Ritchie, D.M., 1988. The C Programming Language.

Kohn, T.A., Essen-Gustavsson, B., Myburgh, K.H., 2007. Exercise pattern influences skeletal muscle hybrid fibers of runners and nonrunners. Med. Sci. Sports Exerc. 39, 1977–1984.

Larsson, L., Moss, R.L., 1993. Maximum velocity of shortening in relation to myosin isoform composition in single fibers from human skeletal-muscles. J. Physiol. 472, 595–614.

Lieber, R.L., 1992. Skeletal Muscle Structure and Function. Williams and Wilkins, Baltimore.

Lieber, R.L., Friden, J., 2000. Functional and clinical significance of skeletal muscle architecture. Muscle Nerve 23, 1647–1666.

Lindstedt, S.L., Hoppeler, H., Bard, K.M., Thronson, H.A., 1985. Estimate of muscle-shortening rate during locomotion. Am. J. Physiol. 249, R699–R703.

Lionikas, A., Li, M., Larsson, L., 2006. Human skeletal muscle myosin function at physiological and non-physiological temperatures. Acta Physiol. 186, 151–158.

MacIntosh, B.R., Bryan, S.N., 2002. Potentiation of shortening and velocity of shortening during repeated isotonic tetanic contractions in mammalian skeletal muscle. Pflugers Arch. 443, 804–812.

MacIntosh, B.R., Neptune, R.R., Horton, J.F., 2000. Cadence, power, and muscle activation in cycle ergometry. Med. Sci. Sports Exerc. 32, 1281–1287.

Marden, J.H., Fitzhugh, G.H., Girgenrath, M., Wolf, M.R., Girgenrath, S., 2001. Alternative splicing, muscle contraction and intraspecific variation: associations between troponin T transcripts, Ca2+ sensitivity and the force and power output of dragonfly flight muscles during oscillatory contraction. J. Exp. Biol. 204, 3457–3470.

Marsh, R.L., 1988. Ontogenesis of contractile properties of skeletal muscle and sprint performance in the lizard Dipsosaurus dorsalis. J. Exp. Biol. 137, 119–139.

Marsh, R.L., 1990. Deactivation rate and shortening velocity as determinants of contractile frequency. Am. J. Physiol. 259, R223–R230.
Marsh, R.L., 1999. How muscles deal with real-world loads: the influence of length trajectory on muscle performance. J. Exp. Biol. 202, 3377–3385.
Marsh, R.L., Olson, J.M., 1994. Power output of scallop adductor muscle during contractions replicating the in vivo mechanical cycle. J. Exp. Biol. 193, 139–156.
Martin, J.C., 2007. Muscle power: the interaction of cycle frequency and shortening velocity. Exerc. Sport Sci. Rev. 35, 74–81.
Marx, J.O., Olsson, M.C., Larsson, L., 2006. Scaling of skeletal muscle shortening velocity in mammals representing a 100,000-fold difference in body size. Pflugers Arch. 452, 222–230.
McCartney, N., Heigenhauser, G.J.F., Jones, N.L., 1983. Power output and fatigue of human muscle in maximal cycling exercise. J. Appl. Physiol. 55, 218–224.
McMahon, T.A., 1975. Using body size to understand structural design of animals – quadrupedal locomotion. J. Appl. Physiol. 39, 619–627.
Medler, S., 2002. Comparative trends in shortening velocity and force production in skeletal muscles. Am. J. Physiol., Regul. Integr. Comp. Physiol. 283, R368–R378.
Medler, S., Lilley, T., Mykles, D.L., 2004. Fiber polymorphism in skeletal muscles of the American lobster, Homarus americanus: continuum between slow-twitch (S-1) and slow-tonic (S-2) fibers. J. Exp. Biol. 207, 2755–2767.
Minetti, A.E., Capelli, C., Zamparo, P., Diprampero, P.E., Saibene, F., 1995. Effects of stride frequency on mechanical power and energy expenditure of walking. Med. Sci. Sports Exerc. 27, 1194–1202.
Mizisin, A.P., Josephson, R.K., 1987. Mechanical power output of locust flight muscle. J. Comp. Physiol. 160A, 413–419.
Pabst, D.A., 1996. Springs in swimming animals. Am. Zool. 36, 723–735.
Packard, G.C., Boardman, T.J., 1999. The use of percentages and size-specific indices to normalize physiological data for variation in body size: wasted time, wasted effort? Comp. Biochem. Physiol. A 122, 37–44.
Parcell, A.C., Sawyer, R.D., Poole, C.R., 2003. Single muscle fiber myosin heavy chain distribution in elite female track athletes. Med. Sci. Sports Exerc. 35, 434–438.
Pearson, S.J., Cobbold, M., Orrell, R.W., Harridge, S.D.R., 2006. Power output and muscle myosin heavy chain composition in young and elderly men. Med. Sci. Sports Exerc. 38, 1601–1607.
Pellegrino, M.A., Canepari, M., Rossi, R., D'Antona, G., Reggiani, C., Bottinelli, R., 2003. Orthologous myosin isoforms and scaling of shortening velocity with body size in mouse, rat, rabbit and human muscles. J. Physiol. 546, 677–689.
Perry, M.J., Tait, J., White, S.C., Medler, S., in press. Skeletal muscle fiber types in the ghost crab, *Ocypode quadrata:* implications for running performance. J. Exp. Biol.
Pette, D., 2002. The adaptive potential of skeletal muscle fibers. Can. J. Appl. Physiol. 27, 423–448.
Reggiani, C., Bottinelli, R., Stienen, G.J.M., 2000. Sarcomeric myosin isoforms: fine tuning of a molecular motor. News Physiol. Sci. 15, 26–33.
Rome, L.C., Lindstedt, S.L., 1997. Mechanical and metabolic design of the muscular system in vertebrates. Handbook of Physiology, Section 13. Comparative Physiology, vol. 13. American Physiological Society, Bethesda, MD, pp. 1587–1651.
Rome, L.C., Funke, R.P., Alexander, R.M., Lutz, G., Aldridge, H., Scott, F., Freadman, M., 1988. Why animals have different muscle fibre types. Nature 335, 824–827.
Rome, L.C., Syme, D.A., Hollingworth, S., Lindstedt, S.L., Baylor, S.M., 1996. The whistle and the rattle: The design of sound producing muscles. Proc. Natl. Acad. Sci. U. S. A. 93, 8095–8100.
Sargeant, A.J., 2007. Structural and functional determinants of human muscle power. Exp. Physiol. 92, 323–331.
Schiaffino, S., Reggiani, C., 1996. Molecular diversity of myofibrillar proteins: gene regulation and functional significance. Physiol. Rev. 76, 371–423.
Shiels, H.A., Stevens, E.D., Farrell, A.P., 1998. Effects of temperature, adrenaline and ryanodine on power production in rainbow trout Oncorhynchus mykiss ventricular trabeculae. J. Exp. Biol. 201, 2701–2710.
Stephenson, G.M., 2001. Hybrid skeletal muscle fibres: a rare or common phenomenon? Clin. Exp. Pharmacol. Physiol. 28, 692–702.
Stroustrup, B., 1987. The C++ Programming Language. Addison-Wesley, Reading, Mass.
Swoap, S.J., Caiozzo, V.J., Baldwin, K.M., 1997. Optimal shortening velocities for in situ power production of rat soleus and plantaris muscles. Am. J. Physiol. Cell.Physiol. 42, C1057–C1063.
Swoap, S.J., Johnson, T.P., Josephson, R.K., Bennett, A.F., 1993. Temperature, muscle power output and limitations on burst locomotor performance of the lizard Dipsosaurus dorsalis. J. Exp. Biol. 174, 185–197.
Syme, D.A., Shadwick, R.E., 2002. Effects of longitudinal body position and swimming speed on mechanical power of deep red muscle from skipjack tuna (Katsuwonus pelamis). J. Exp. Biol. 205, 189–200.
Tobalske, B.W., Dial, K.P., 2000. Effects of body size on take-off flight performance in the Phasianidae (Aves). J. Exp. Biol. 203, 3319–3332.
Turvey, M.T., Schmidt, R.C., Rosenblum, L.D., Kugler, P.N., 1988. On the time allometry of coordinated rhythmic movements. J. Theor. Biol. 130, 285–325.
Van Wassenbergh, S., Herrel, A., James, R.S., Aerts, P., 2007. Scaling of contractile properties of catfish feeding muscles. J. Exp. Biol. 210, 1183–1193.
Wakeling, J.M., 2005. Motor unit recruitment during vertebrate locomotion. Anim. Biol. 55, 41–58.
Wakeling, J.M., Johnston, I.A., 1998. Muscle power output limits fast-start performance in fish. J. Exp. Biol. 201, 1505–1526.
Weis-Fough, T., Alexander, R.M., 1977. The sustained power output from striated muscle. In: Pedley, T.J. (Ed.), Scale Effects in Animal Locomotion. Academic Press, London, pp. 511–525.
Williamson, D.L., Pallagher, P.M., Carroll, C.C., Raue, U., Trappe, S.W., 2001a. Reduction in hybrid single muscle fiber proportions with resistance training in humans. J. Appl. Physiol. 91, 1955–1961.
Williamson, M.R., Dial, K.P., Biewener, A.A., 2001b. Pectoralis muscle performance during ascending and slow level flight in mallards (Anas platyrhynchos). J. Exp. Biol. 204, 495–507.
Young, I.S., Rome, L.C., 2001. Mutually exclusive muscle designs: the power output of the locomotory and sonic muscles of the oyster toadfish (Opsanus tau). Proc. R. Soc. Lond. B. Biol. Sci. 268, 1965–1970.